https://doi.org/10.5194/wcd-2023-6
Preprint. Discussion started: 21 February 2023

Weather and Climate Dynamics Discussions
Open Access
EGU

Strengthening gradients in the tropical west Pacific connect to European summer temperatures on sub-seasonal timescales

Chiem van Straaten[1,2], Dim Coumou[1,2], Kirien Whan[1], Bart van den Hurk[2,3], and Maurice Schmeits[1,2]

[1]Royal Netherlands Meteorological Institute (KNMI), De Bilt, the Netherlands
[2]Institute for Environmental Studies (IVM), Vrije Universiteit Amsterdam, Amsterdam, the Netherlands
[3]Deltares, Delft, the Netherlands

Correspondence: Chiem van Straaten (j.w.vanstraaten@vu.nl)

Abstract. Recent work has shown that (sub-)seasonal variability in tropical Pacific convection, closely linked to ENSO, relates to summertime circulation over the Euro-Atlantic. The teleconnection is non-stationary, probably due to long-term changes in both the tropical Pacific and extra-tropical Atlantic. It also appears imperfectly captured by numerical models. In a previous study we found that the best predictor of errors in sub-seasonal forecasts of European temperature, is a dipole in tropical west Pacific sea surface temperatures (SSTs). In this diagnostic study we use reanalysis data to further investigate the teleconnection pathway and the processes behind its non-stationarity. We show that SST gradients associated with the dipole represent a combination of ENSO variability and west Pacific warming, and have become stronger since 1980. Associated patterns of suppressed and enhanced tropical heating are followed by quasi-stationary waves that linger for multiple weeks. Situations with La Niña-like gradients are followed by high pressure centers over eastern Europe and Russia, three to six weeks later. Inverted situations are followed by high pressure over western Europe, three to six weeks later. The latter situation is however also conditional on a strong meridional tripole in north Atlantic SST and a co-located jet stream. Overall, the sub-seasonal pathway diagnosed in this study connects to patterns detected at seasonal scales, and confirms earlier findings that the summertime connectivity between the Pacific and Europe has shifted in recent decades. It also partly explains the increased occurrence of high sea level pressures and summer temperatures over the European continent.

1 Introduction

Sub-seasonal forecasts are made with a lead time of 2-6 weeks. For weather at any mid-latitude location, part of the predictability at that lead time originates in the tropics (Vitart and Robertson, 2018). Tropical deep convection and associated diabatic heating generate upper level divergence and vorticity anomalies that force Rossby Waves (Hoskins and Karoly, 1981; Sardeshmukh and Hoskins, 1988; Trenberth et al., 1998). These waves can propagate into the westerly mid-latitude flow and steer associated weather patterns, commonly taking two weeks to establish (Liu and Alexander, 2007; Branstator, 2014; Stan et al., 2017). Impacts on mid-latitude surface weather are especially pronounced when waves are quasi-stationary (Schubert et al., 2011; Wolf et al., 2018; Röthlisberger et al., 2019). An example of a teleconnection from tropical heating is the Madden Julian Oscillation, which in the Euro-Atlantic sector, has a phase-dependent influence on the North Atlantic Oscillation (Cassou, 2008; Henderson et al., 2017; Vitart, 2017).

https://doi.org/10.5194/wcd-2023-6
Preprint. Discussion started: 21 February 2023

Since its origins, teleconnection research has mostly focused on winter, as this is a season with higher baroclinicity and more potent Rossby wave propagation (Bjerknes, 1969; Trenberth et al., 1998; Branstator and Teng, 2017). Teleconnections are also thought to have an influence in summer (Cassou et al., 2005). Heating patterns over the western tropical Pacific are of primary importance for summertime quasi-stationary Rossby waves (QSRWs) (Ting, 1994; Behera et al., 2013; Ma and Franzke, 2021). The dipole of enhanced convective activity over the Maritime continent, in conjunction with reduced activity over the west and central Pacific is related to circulation over the Euro-Atlantic sector (O'Reilly et al., 2018; Fuentes-Franco and Koenigk, 2020). One feature known for producing such contrasts in sea surface temperature (SST) and atmospheric heating, is the El Niño Southern Oscillation (ENSO). When ENSO's atmospheric component (the Walker circulation) strengthens, convection over the Maritime continent increases and that over the tropical central Pacific decreases (Bjerknes, 1969). Such a (developing) La Niña episode was found to have supported the prominent blocking that was part of the Russian heatwave of 2010 (Schneidereit et al., 2012).

Such an ENSO-induced contrast in convection over tropical central Pacific and Maritime continent, is oriented along the equator. Diagnosis of heating differentials also reveals that meridional contrasts have a role in steering mid-latitude flow (Ding et al., 2011). Such contrasts reflect activity of the Indian Summer Monsoon, and the western north Pacific monsoon. Both meridional and equatorial SST contrasts have increased rapidly since 1990 by what is called the 'west Pacific warming mode' (Funk and Hoell, 2015). It consists of concentrated warming over the Maritime continent and the western north Pacific (WNP). This is found to be a response to anthropogenic emissions (Funk and Hoell, 2015) and has strengthened the Walker circulation (Funk et al., 2018; Lee et al., 2022).

Coinciding with west Pacific warming, observed connectivity between the Pacific and Euro-Atlantic circulation appears to have strengthened (O'Reilly et al., 2019; Sun et al., 2022). This strenthening is not a conseqeuence of internal amospheric variability but is a response to the SST trends (O'Reilly et al., 2019), potentially influencing current and future Euro-Atlantic circulation. Unfortunately, numerical climate models seem unable to reproduce the observed changes in Euro-Atlantic circulation (Boe et al., 2020), meaning they underestimate the rapid increase of European summer temperature extremes (van Oldenborgh et al., 2022). Also numerical weather prediction (NWP) models have shortcomings in simulating Rossby Wave teleconnections (O'Reilly et al., 2018; Quinting and Vitart, 2019). We previously found that west Pacific SSTs could relate to QSRWs that conditionally led to monthly European summer temperature anomalies. This teleconnection appeared imperfectly represented in the numerical model of the European Center for Medium-range Weather Forecasts (ECMWF) (van Straaten et al., 2023).

The shortcomings of weather- and climate-models can reside in many processes associated with Rossby Wave teleconnections. Whether QSRWs influence a remote location can be modulated by processes related to the forcing of waves, and processes related to wave propagation and amplification (White et al., 2022). In the Pacific region, or further along the propagation trajectory, other sources of heating and vorticity can strengthen the QSRW when they are in-phase, and negate it when they are out-of-phase, dependent on the optimal forcing pattern of the QSRW (Schubert et al., 2011; Kim and Lee, 2022). Extra-tropical Pacific SST anomalies provide such feedback when preceding dynamics have left in place an anomaly pattern that is in-phase with a summertime QSRW (Vijverberg and Coumou, 2022). In the same way the state of the north Atlantic can

https://doi.org/10.5194/wcd-2023-6
Preprint. Discussion started: 21 February 2023

permit or hinder QSRW propagation towards Europe (Fuentes-Franco et al., 2022). Also soil moisture depletion, for example over the US, can amplify wave patterns and make them circumglobal (Teng and Branstator, 2019).

A second potential modulator is the way atmospheric jets function as waveguides (Hoskins and Ambrizzi, 1993; White et al., 2022). Waveguides are sharp gradients in the background flow, along which Rossby Waves propagate (Wirth et al., 2018; Manola et al., 2013). The role of jets is noticable as strong waves often emanate at their exit regions, of which the Euro-Atlantic sector is one (Stan et al., 2017). The characteristics of the background flow, in the form of jet position, width and strength can determine whether a wave response will be of limited longitudinal extent, or circumglobal (Branstator and Teng, 2017).

In this study we want to characterize the west Pacific to Europe teleconnection and evaluate if changes in the Pacific, and associated strengthening of the connection can indeed be an explanation of observed Euro-Atlantic circulation changes. To that end we build an index for SST dipoles over the west Pacific, and an index for European surface temperature more than two weeks later. Such a lagged, sub-seasonal timeframe is different from the concurrent, seasonal diagnostics used in earlier studies (Ding et al., 2011; Behera et al., 2013; O'Reilly et al., 2018). We examine the pathway between the two end-points, and investigate whether the pathway is modulated by (a combination of) the processes described above. Such modulation might explain the conditional sub-seasonal occurrence. Overall, we hope that our characterization can help in targeting weather- and climate-model evaluations, such that long term projections and sub-seasonal forecasts of European summer extremes can be improved.

2 Data

In this study we use the ERA5 reanalysis (Hersbach et al., 2020). We extract daily values of sea surface temperature (SST) and two-meter temperature (t2m), as they will form the respective start- and end-point of the teleconnection. Top-of the atmosphere outgoing longwave radiation (OLR) was extracted as indicator of tropical deep convection, zonal wind at 300 hPa (u300) as an indicator of jet stream strength and position, and geopotential height at 300 hPa (z300) as an indicator of the QSRW itself. Values were extracted from 1950 until 2021, in a domain that spans from 20°S to 90°N, and 180°W to 180°E, at a spatial resolution of 0.25x0.25°.

Daily values were de-seasonalized by approximating the seasonal cycle with a polynomial that is a function of the day-in-the year (as in Mayer and Barnes, 2021, 2022). We found that a 7-degree polynomial was most suited to accomodate the changing shape of seasonal cycles with latitude. At polynomials below 5 degrees the residuals remained visibly dependent on the season. For each gridcell the polynomial was fitted to the complete set of years from 1950 till 2021. Daily anomalies were then averaged to four-week (31-day) values for t2m and three-week (21-day) values for the other variables. In previous studies we namely found that three-week averages of SST and other variables are at least as related to four-week European t2m as four-week averages (van Straaten et al., 2022, 2023). Both aggregations were executed as a rolling-window averaging, such that one value was recorded each day

https://doi.org/10.5194/wcd-2023-6
Preprint. Discussion started: 21 February 2023

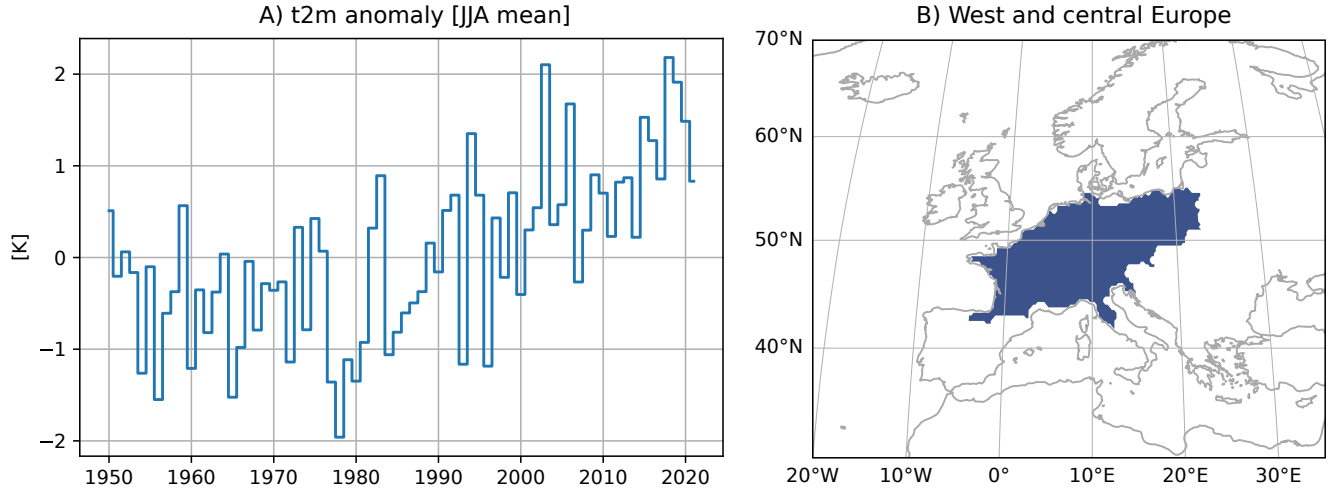

Figure 1. Two-meter temperature (t2m) anomaly in west and central Europe. A) Seasonal mean (JJA) ERA5 t2m anomaly in the region, from 1950 to 2021. B) west and central European region.

The western north Pacific (WNP) region, whose warming as part of the west Pacific warming mode was found to have strong influence on the Walker Circulation, is defined from 10°N–30°N 130°E–170°W (Funk et al., 2018). In this region we record each day the spatial mean, three-week average SST anomaly.

To investigate the role of ENSO we use pre-computed monthly relative ENSO indices (van Oldenborgh et al., 2021), based on the ersstv5 dataset of ocean observations (Huang et al., 2017), in regions Niño 3 and Niño 4 (Trenberth and Stepaniak, 2001). Relative ENSO indices are defined relative to the global average SST between 20°N and 20°S, which makes them less distorted by global warming. We interpolate them linearly to obtain a monthly value each day.

For the Pacific Decadal Oscillation (PDO) we use standardized values of the first principle component of monthly Pacific SST anomalies north of 20°N (Mantua et al., 1997). The pre-computed index is provided by NOAA, is based on ersstv5, and has the global mean sst anomaly subtracted to make it less distorted by global warming. We interpolate the PDO index linearly to obtain a monthly value each day.

The sub-seasonal predictand is derived from gridded t2m through spatial and temporal aggregation. This is required to capture the overarching variability that affects daily anomalies at multiple moments and locations. When prediction is attempted for individual samples, the variability would be harder to detect and harder to predict with sub-seasonal lead times (Buizza and Leutbecher, 2015; Wheeler et al., 2017; van Straaten et al., 2020). In a previous study we used hierarchical clustering to find a west and central European region (Fig. 1B), in which the average t2m anomaly is predictable when also aggregated to the four-week or monthly time scale (van Straaten et al., 2022). Using rolling averages as described above, we thus create a four-week average response variable which we will refer to as ‘t2m in week 3,4,5 and 6’. A diagnostic plot of June-July-August (JJA) averages of this variable shows that summer temperatures have been warming. In fact, western Europe has been warming faster than the global average (Christidis et al., 2015), especially since the 1990’s.

https://doi.org/10.5194/wcd-2023-6
Preprint. Discussion started: 21 February 2023

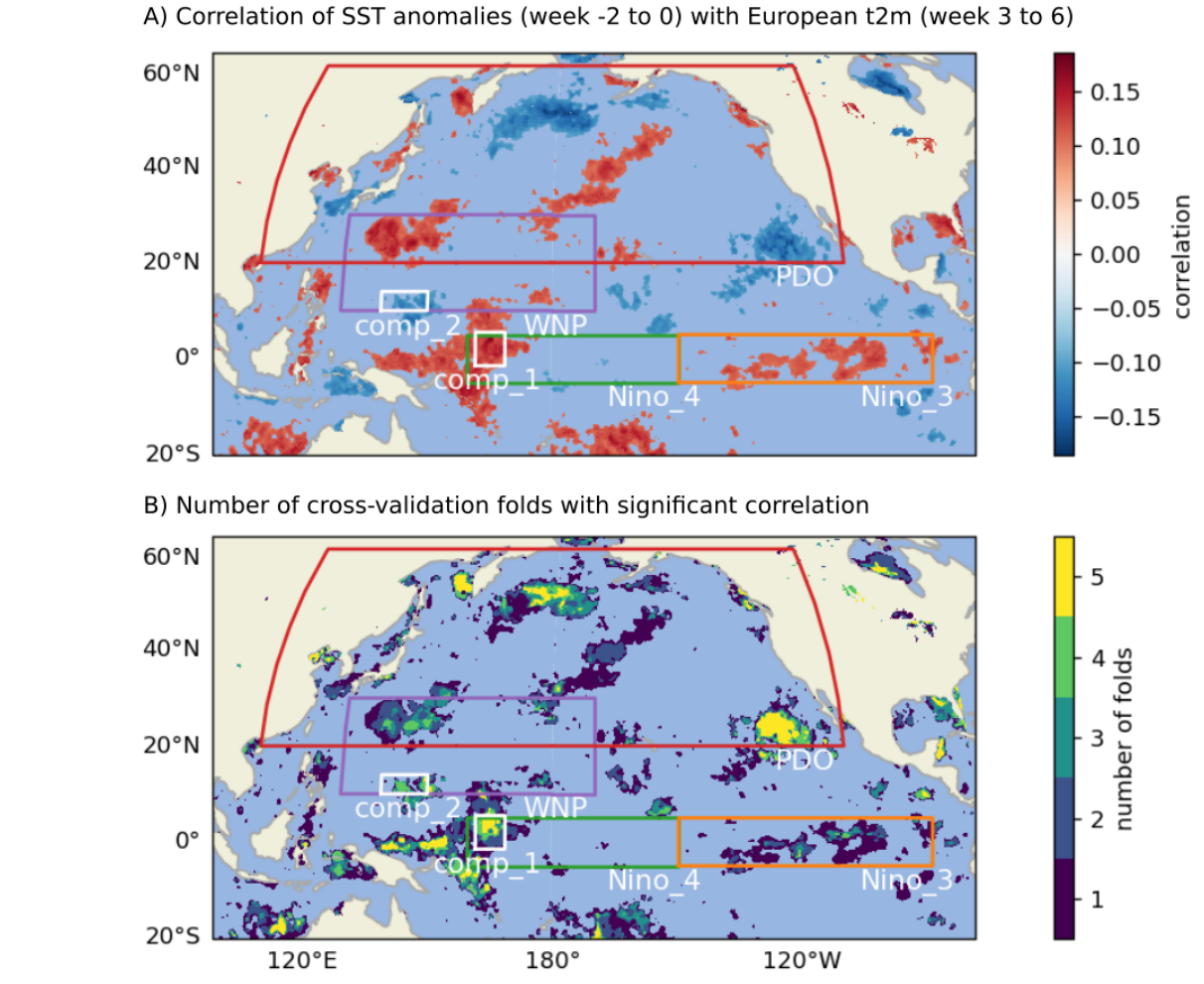

Figure 2. Connection between ERA5 Pacific SST anomalies and European t2m anomalies at sub-seasonal timescales in summer (1950-2021). A) Spearman rank correlation between week -2 to 0 SST anomalies and week 3 to 6 western European t2m, corrected for inflation by linear trends, seasonality and auto-correlation. Reported is the mean correlation over 5 crossvalidation folds, constructed by leaving out consecutive blocks of 14 years. B) Robustness of the correlation as measured by the number of folds with significant correlation. Annotated are regions commonly used to capture Pacific variability. The two components of the west Pacific Dipole (WPD) index are highlighted by white squares.

3 West Pacific dipole index

Figure 2 displays Pacific SST grid-cells whose variability precedes European t2m by more than two weeks. We correlate three-week-average SST anomalies ('SST in week -2 to 0') to lagged European four-week-averaged t2m in week 3 to 6, while correcting for factors inflating the correlation, like global warming and auto-correlation (Fig. 2A). Specifically, we compute the
115 partial correlation between residual SST and residual t2m. Those residuals remain after a linear regression predicts observed

https://doi.org/10.5194/wcd-2023-6
Preprint. Discussion started: 21 February 2023

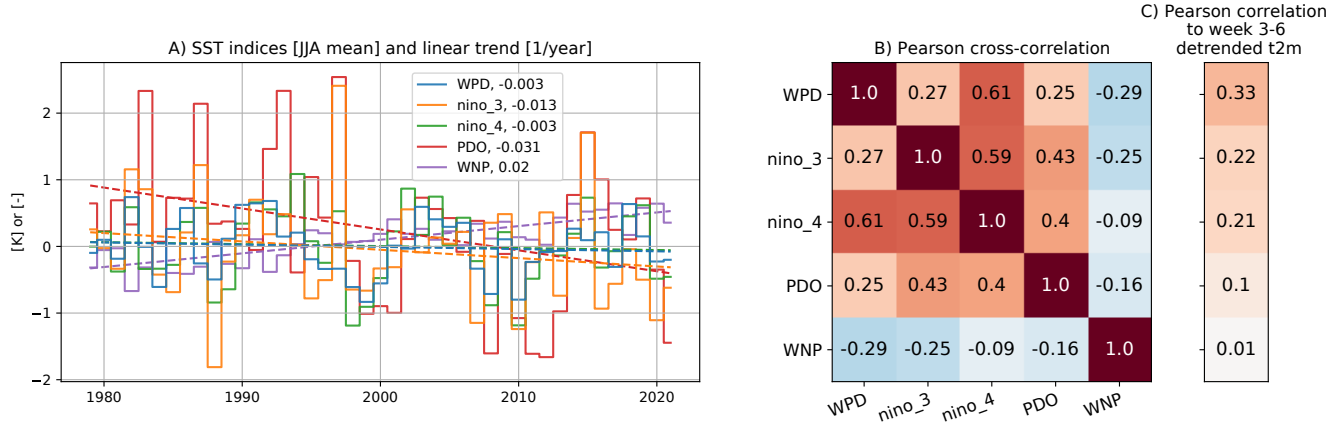

Figure 3. Correspondence between the west Pacific Dipole index (WPD: SST in 'component_1' minus SST in 'component_2', Fig. 2), and other Pacific indices. A) Seasonal mean timeseries and linear trend from 1979 till 2021. B) Cross-correlation matrix between the SST indices (JJA only). C) Lagged correlation between SST indices and European t2m in week 3 to 6, corrected for a linear trend in t2m. The SST indices capture SSTs from week -2 to 0 for WPD and WNP, and SSTs from week -3 to 0 for PDO and Niño (see also section 2).

SST and t2m anomalies using time and the value of the previous timestep (details can be found in van Straaten et al., 2022). Within the full dataset of 1950 to 2021, we test robustness of the partial correlation with a five-fold crossvalidation, leaving out consecutive blocks of 14 years. Grid cells with correlations significantly different from zero in five out of five subsets are highlighted in yellow (Fig. 2B) ($\alpha = 5 \cdot 10^{-12}$, corrected for the false discovery rate (Benjamini and Hochberg, 1995)).

The highlighted SST regions relate to European t2m, and do not correspond perfectly to patterns that explain the highest amount of Pacific variability, like PDO and ENSO. Aspects are however captured. A large cluster of significant cells resides in the region used to define the PDO (Mantua et al., 1997) (Fig. 2B). Also at the eastern edge of the Niño 4 area we see a cluster of cells (called 'component 1'). This cluster is flanked by 'component 2' which lies at 10°N in the WNP area (Fig. 2). The respective positive and negative correlations of component 1 and 2 (Fig. 2A), hint at situations with anomalously warm SSTs in component 1 and anomalously cold SSTs in component 2, and in which week 3 to 6 European t2m would later be above normal (and vice-versa). With component 2 located in the WNP, and component 1 at the western edge of the central Pacific, their combination appears to capture the combined equatorial and meridional heating contrast known to force a teleconnection towards Europe (Ding et al., 2011; Behera et al., 2013; O'Reilly et al., 2018; Ma and Franzke, 2021). In van Straaten et al. (2023) the contrast was captured with a spatial co-variance predictor and was found to relate to a failure of the ECMWF model to represent the teleconnection. Here we simply capture the contrast by defining a west Pacific Dipole (WPD) index, namely the three-week anomaly in component 1 minus the three-week anomaly in component 2. As SSTs in the tropical west Pacific are, in absolute terms, generally warmer than those in the tropical central Pacific, this definition dictates that: positive WPD values represent a weaker equatorial SST gradient, and negative WPD values represent a stronger equatorial gradient. The reason that positive WPD is defined as 'positive', is its association to above-normal western European t2m (Fig. 3C).

https://doi.org/10.5194/wcd-2023-6
Preprint. Discussion started: 21 February 2023

Weather and Climate Dynamics Discussions
Open Access
EGU

We expect the WPD index to relate to other Pacific modes. PDO for instance, comprises a combination of remote ENSO-induced variability in combination with local atmosphere-ocean interactions (Newman et al., 2016). Especially due to spatial overlap in regions, we see that WPD relates to Niño 4 and WNP, which is illustrated by cross-correlations of 0.61 and -0.29 respectively, in the period from 1979 until 2021 (Fig. 3B). We do not include the pre-1979 period because it lacks the west Pacific warming mode and the stronger Pacific-Atlantic connections (Funk and Hoell, 2015; O'Reilly et al., 2019), which would muddy the illustration of current inter-relations. The real difference with for instance Niño 4, is that the WPD-index is designed to specifically target the teleconnection towards Europe, which is confirmed by the highest correlation of all indices to week 3-6 t2m (Fig. 3C).

Correlation between Pacific modes is further illustrated by a year-to-year representation of the time series (Fig. 3A). Over the 1979-2021 period the standardized PDO is moving towards a negative phase (-0.031 std/yr). Also Niño 3 displays a slight negative trend (-0.013 K/yr), which is different from Niño 4 and WPD, and opposed to the positive trend in WNP (0.02 K/yr). These opposing trends reflect documented warming in the western Pacific, while the central to eastern tropical Pacific has not warmed, and has thus seen a relative cooling (Wills et al., 2022; Seager et al., 2022; Sun et al., 2022; Lee et al., 2022). The result is an increase of equatorial and meridional gradients, and Pacific SST states that are more 'La Niña-like', with a stronger Walker circulation (Funk and Hoell, 2015; Lee et al., 2022), and potentially important influences on tropical-extratropical teleconnections (Schubert et al., 2014; O'Reilly et al., 2019; Sun et al., 2022).

4 Emergence of a teleconnection

We classify the WPD index into three tercile-based categories. The positive phase is when SSTs during week -2 to 0 are anomalously warm in component 1 and anomalously cold in component 2. In the negative phase this is inverted, and a neutral phase is in-between. Because the WPD index does not have a significant trend (Fig. 3A, -0.003 K/yr), we determine tercile thresholds over the entire 1950-2021 dataset. For week 3-to-6 t2m on the other hand, tercile thresholds are computed per rolling window of 21 summers. Otherwise the large trend (Fig. 1A) would fill the 'positive' class mostly with samples from recent years. This would distort the lagged t2m response that forms part of our measure of teleconnection strength: namely the number of occasions with (i) *positive WPD* AND *positive t2m response*, plus the number of occasions with (ii) *negative WPD* AND *negative t2m response*.

Temporal evolution of the WPD classes reveals that since 1950 (the beginning of the dataset) the negative WPD phase has strongly increased in frequency (blue line in Fig. 4A). Until 2000 this happens mostly at the expense of the neutral phase, and after that also at the expense of the positive phase. The dwindling occurrence of the neutral phase can explain why the tercile distribution shows large changes (Fig. 4A), whereas the seasonal mean of WPD had no signficant trend (Fig. 3A). The increased occurrence of negative WPD phases does agree with WNP warming and the strengthening of equatorial gradients over the Pacific (Section 3, Fig. 3A).

Concurrent with this development we see that lagged t2m phases in week 3 to 6 increasingly follow the WPD phases in week -2 to 0. The sum of positive and negative responses to respectively, positive and negative WPD, rises beyond values found by

https://doi.org/10.5194/wcd-2023-6
Preprint. Discussion started: 21 February 2023

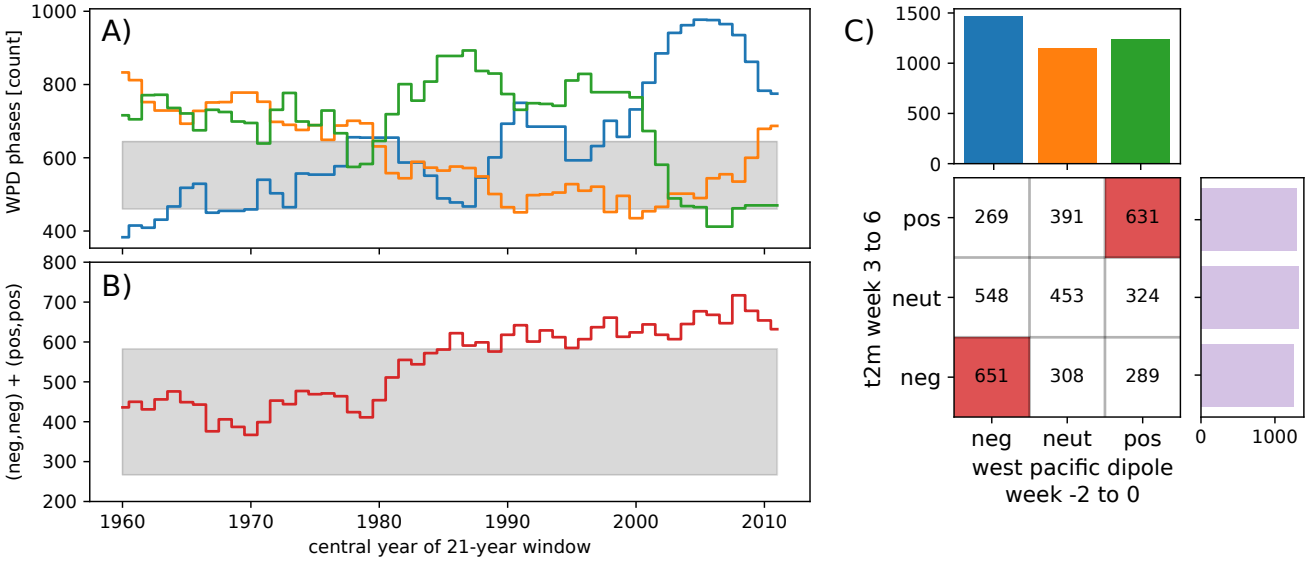

Figure 4. Teleconnection between week -2 to 0 west Pacific Dipole index and week 3-6 European t2m, as measured by correspondence in tercile classes (negative, neutral, positive). A) Prevalence of the three WPD classes in a moving window of 21 summer seasons (blue: negative WPD; orange: neutral WPD; green: positive WPD), with tercile thresholds determined over the entire dataset, from 1950-2021. B) Total occurrence of the negative and positive phase of the teleconnection, i.e. a negative WPD preceding a negative t2m response plus a positive WPD preceding a positive t2m response, as counted for each 21-season window, whereby the t2m tercile thresholds are re-computed in each window. Grey areas in (A) and (B) denote the 0.025 and 0.975 quantiles of the uncertainty distribution when counting is performed on 21 summer seasons that are randomly sampled from the 1950-2021 dataset (500 repeats, with replacement). C) Distribution of tercile classes for WPD (x-axis) and European t2m (y-axis) as counted for each 21-season window from 1980 till 2021 (central years 1990-2011) when the teleconnection (both in negative and positive phase) was present in a statistically significant way (as shown in panel B).

chance (grey area, Fig. 4B). This roughly occurs for 21-year windows centered in 1990 and beyond, meaning it starts in 1980. The emergence of a significant teleconnection between the Pacific and Euro-Atlantic circulation is reported by other studies, both for the past decades (Wu and Lin, 2012; Lim et al., 2019; O'Reilly et al., 2019; Sun et al., 2022), and for the near-future (Mayer and Barnes, 2022).

In the remainder of this paper we focus on the period 1980-2021 in which a significant teleconnection has emerged. The joint distribution of WPD and t2m phases is given in Figure 4C. Presented are the number of samples in each category (3- and 4-week averages for WPD and t2m respectively, with values recorded each day). Note that the marginal distribution of t2m is uniform, because tercile thresholds are re-estimated in each rolling 21-year window, and that the marginal of WPD is not uniform and shows the relative dominance of negative WPD phases in this period.

https://doi.org/10.5194/wcd-2023-6
Preprint. Discussion started: 21 February 2023

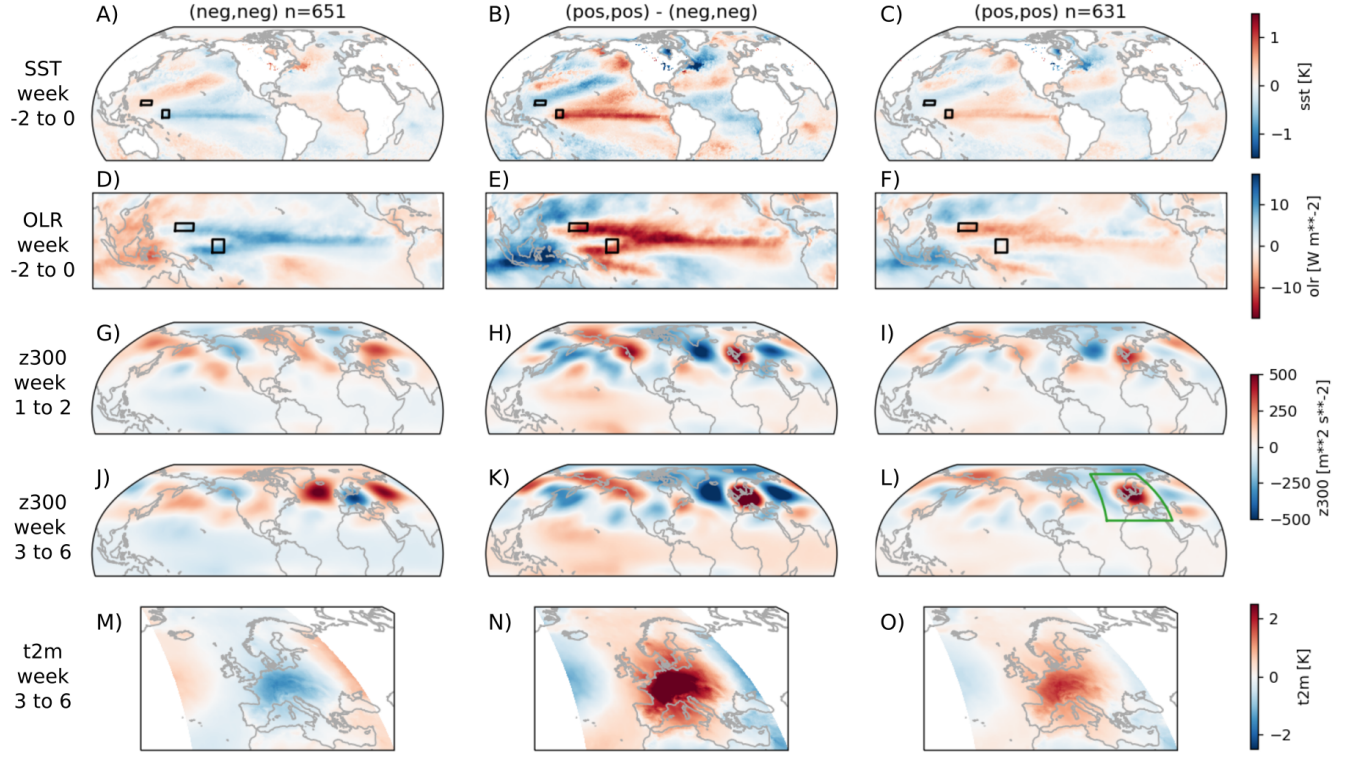

Figure 5. Composite plots illustrating the teleconnection between week -2 to 0 west Pacific SST and week 3 to 6 west-central European t2m, based on composite anomalies from the period 1980-2021 (climate normal also estimated from 1980-2021). Left column: Samples in which negative WPD phases precede the negative t2m class (n=651). Right column: Samples in which positive WPD phases precede the positive t2m class (n=631). Middle column: Difference between panels in the right and left column. From top to bottom: SST pattern and OLR in week -2 to 0, the subsequent z300 response in week 1 and 2, and the eventual impact on z300 and surface temperature in week 3 to 6. Black insets in panels A-F show the two components of the West Pacific Dipole index. Green inset in panel L serves as reference for the spatial extent of surface t2m in the bottom row.

5 Forcing, quasi-stationary wave, and surface imprint

We now investigate the spatial and temporal patterns that occur during the period that the teleconnection is significant. Different components of the pathway (i.e. SST, OLR, z300, t2m) are plotted as rows in Figure 5. The negative phase, positive phase and their difference are plotted in the left, right and middle column, respectively.

It is clear that the WPD index captures a large geographical pattern with pronounced SST and OLR anomalies accross the Pacific ocean, despite being defined by small boxes (Fig. 5A-F). Visually, the SST states in week -2 to 0 represent a combination of three patterns: (i) ENSO, which is visible in the La-Niña-like equatorial contrast between anomalously cool SSTs in Niño 4 and anomalously hot SSTs around the Maritime continent in Fig. 5A, and in the El-Niño-like contrasts in Fig. 5C, (ii) the west Pacific warming mode, which resembles a tilted red 'V' and connects the above-normal SSTs around the Maritime continent to

https://doi.org/10.5194/wcd-2023-6
Preprint. Discussion started: 21 February 2023

the extra-tropics, in north-eastward and south-eastward direction (our Fig. 5A and Fig. 1A of Funk and Hoell (2015)), and (iii) the PDO-like pattern that the north-eastward extension of warm SSTs also resembles, which is known to provide summertime predictability for the eastern US (our Fig. 5A and Fig. 1F of Vijverberg and Coumou (2022)).

In OLR we see that the WPD phases correspond to clear contrasting signals in anomalous deep convection, but that these contrasting signals need not be aligned with the dipole in anomalous SST and the WPD boxes themselves (Fig. 5D-F). The heating during weeks -2 to 0 reflects equatorial contrasts like the enhanced heating over Niño 3 and 4, in combination with reduced heating over the Maritime Continent (Fig. 5F). But OLR also reflects meridional contrasts like increased activity of the western north Pacific monsoon (heating centered around 15°N, east of the Philippenes, in region component 2, Fig. 5F). Both types of heating contrasts were found to be important by Ding et al. (2011). Noteworthy is that the prevalent heating anomaly in the Maritime Continent (either suppressed or enhanced) extends into the Indian ocean (Fig. 5E), confirming that west Pacific forcing is not always separable from forcing in the Indian Ocean (as in Behera et al., 2013; Ma and Franzke, 2021).

The forcing at weeks -2 to 0 translates into an initial atmospheric response in weeks 1-2 (Fig. 5G-I). Centres of action (locations with the largest z300 anomalies) are found from the north Pacific to Eurasia, showing the considerable longitudinal extent of the QSRW (Fig. 5H). Over the north American continent the wave pattern resembles the pattern found by Vijverberg and Coumou (2022) (our Fig. 5H, their Fig. 1b), which here extends towards Europe. The extension involves a prominent center of action south of Greenland, in the north Atlantic, which was also found by O'Reilly et al. (2018). Furthermore, this cyclonic anomaly, in combination with the west/central European high pressure (Fig. 5I), bears similarity to the Summer East Atlantic (SEA) pattern (Fig. 1a of Wulff et al. (2017)). The tropical forcing of SEA was thought to come primarily from the Eastern Pacific and Carribean (Wulff et al., 2017), but our results indicate a possibility of west Pacific forcing as well.

After development in weeks 1 to 2, the lifetime of the QSRW extends into week 3 to 6 (Fig 5J-L). This results in negative t2m anomalies in west and central Europe when WPD was negative and positive t2m anomalies when WPD was positive (Fig 5M,O). In the negative phase a cool western Europe (relative to the climate normal from 1980-2021) is flanked by high pressure and high t2m in Eastern Europe and Russia (Fig. 5J,M). This cold-warm t2m dipole has been reported by earlier studies as well (Behera et al., 2013). In fact, given that the negative phase of WPD is occurring more frequently since 1990 (Fig. 4A), we expect that in recent summers this t2m dipole pattern has become more frequent, which is exactly what Lee et al. (2017) have reported.

6 Modulation

As above, we can look at corresponding WPD and t2m phases and study the teleconnection pathway when it is fully present. But we are also interested in cases where positive or negative WPD phases produce Pacific heating contrasts, but where the full atmospheric response is lacking and the QSRW fails to reach Europe because of a modulating process.

ENSO's influence on the large scale background circulation might be such an indirect modulator (Ding et al., 2011; Schneidereit et al., 2012; O'Reilly et al., 2019). An example is the cooling of the atmosphere in the entire tropical belt by a strong La Niña episode. This changes the zonal mean equator-to-pole gradient and therefore the waveguide (Ding et al., 2011). Modu-

https://doi.org/10.5194/wcd-2023-6
Preprint. Discussion started: 21 February 2023

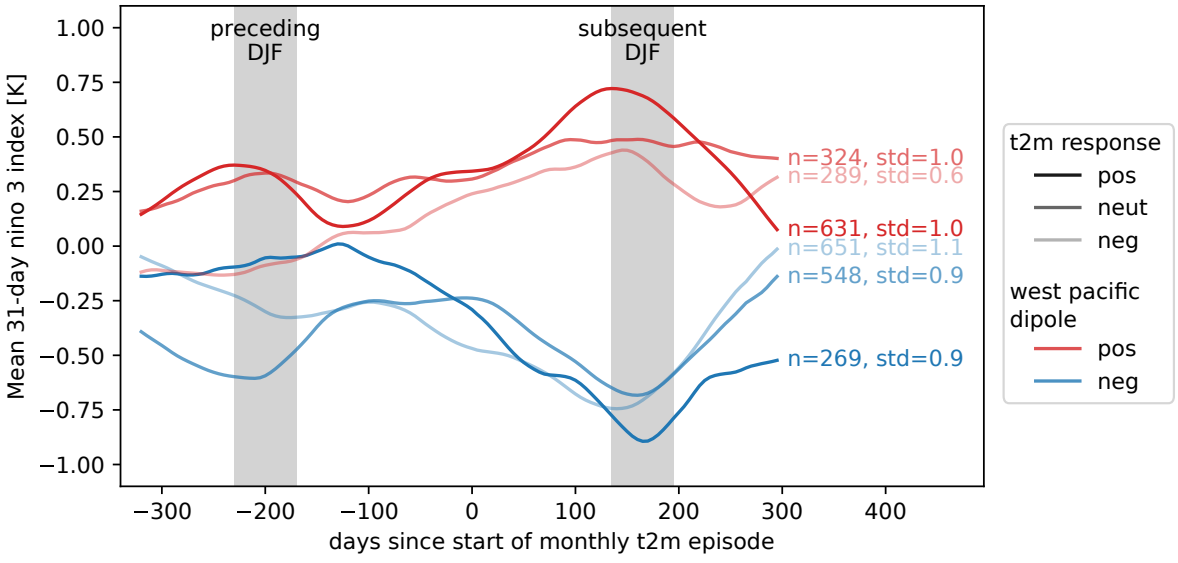

Figure 6. Evolution of the monthly mean relative Niño 3 index, computed per group of samples (determined in JJA). Plotted are groups with positive (red) and negative (blue) WPD phases (based on the SST anomaly in week -2 to 0, sometime in JJA). The phases tend to occur when ENSO evolves from neutral to El Niño or La Niña. Plotted with opacity is the European t2m response in week 3 to 6 (a moment in JJA that we set to zero on the x-axis). This response seems independent of the ENSO state. Samples come from the period 1980-2021. Grey boxes indicate moments that are guaranteed to fall in winter (DJF), as this depends on whether x=0 occurs early or late in summer. Number of samples and standard deviation of DJF values are annotated per group.

lation by ENSO can also happen in a zonally asymmetric way by strengthening the western north Pacific Monsoon, or Indian Summer Monsoon (Ding et al., 2011; Di Capua et al., 2020). The evolution of ENSO, i.e. whether it is strengthening, decaying, or persisting, is important as well (e.g. Jong et al., 2020). Strong expression of a pattern in the preceding winter can namely leave an imprint on extra-tropical SSTs, which leads to favourable or unfavourable diabatic interaction with QSRWs in subsequent seasons (Vijverberg and Coumou, 2022).

We investigate whether positive and negative phases of the summertime teleconnection occur under distinct ENSO evolutions, particularly focusing on ENSO evolution in the central to eastern Pacific (Niño 3) which is less directly related to our WPD index (Fig 3B). Plotted in Figure 6 is the monthly mean evolution of the relative Niño 3 index in each combination of phases (negative WPD phases in blue, positive WPD phases in red, with opacity denoting whether or not we see a European t2m response). As expected, positive and negative WPD phases are El-Niño-like and La-Niña-like, respectively (red lines are generally on top of blue lines, Fig. 6). This differentiation between red and blue actually increases when moving from preceding DJF, via JJA (zero on the x-axis), to subsequent DJF. This suggests that summers with non-neutral WPD phases relate to the strengthening of ENSO: The negative summertime WPD phase occurs during years when ENSO migrates from an average neutral state to a pronounced La Niña state. Vice versa, the positive WPD phase occurs when ENSO migrates from an average

https://doi.org/10.5194/wcd-2023-6
Preprint. Discussion started: 21 February 2023

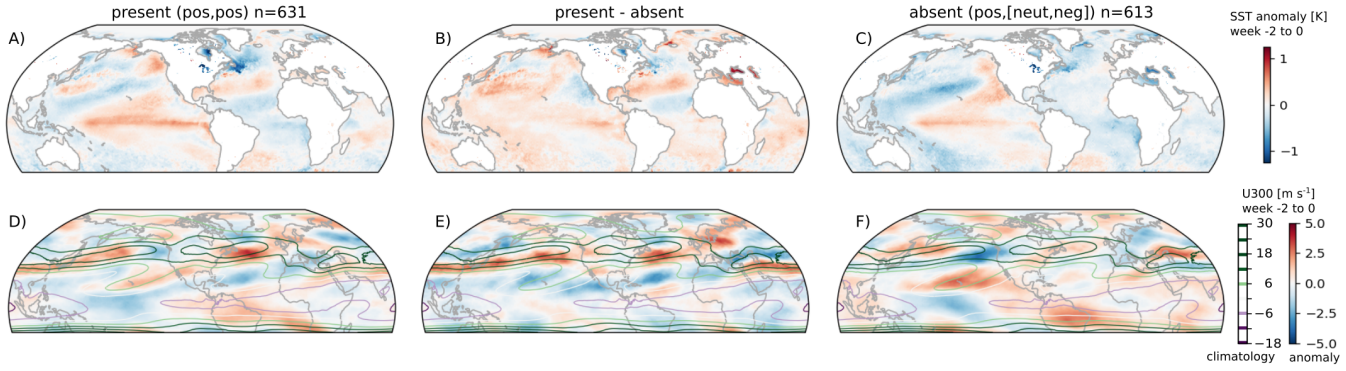

Figure 7. Modulation of the teleconnection when the west Pacific dipole in week -2 to 0 is in its positive phase. Left column: samples with positive t2m response in week 3 to 6, meaning a positive phase teleconnection (n = 631). Right column: samples resulting in a neutral or negative t2m response, meaning an absence of the teleconnection (n = 613). Middle column: difference between panels in the left and right column. Top row: composite anomalies of SST in week -2 to 0. Bottom row: composite U300 anomalies in week -2 to 0. Contour-overlay shows the summertime climatological U300 value. Composites are extracted from the period 1980-2021 (climate normal also defined from 1980-2021).

neutral state to an El Niño state. This does not imply that ENSO also fully determines the resulting t2m response: A negative t2m response is likely after a negative WPD phase (and vice versa) given the significance of the teleconnection (Fig. 4C). But within each WPD group (comparing blue lines of different opacity, and red lines of different opacity), there are no distinct ENSO states related to the 'pos,pos' (darkest red) and 'neg,neg' (lightest blue) teleconnection occurrences (Fig. 6).

If not by ENSO, the QSRWs from west Pacific heating anomalies can also be modulated by other factors. For negative teleconnection phases little was found, but for positive WPD phases we plot the spatial composite patterns of SST and u300 (Fig. 7). The composite plots show the state in week -2 to 0, so before the QSRW occurs, with on the left samples leading to a lagged, positive European t2m response, and on the right all those that do not. The difference plot in the middle column shows that large SST differences are found in the Atlantic (Fig. 7B). A strong meridional cold-warm-cold tripole in the north Atlantic is associated with positive t2m responses (Fig. 7A). Diagnosed by earlier studies, this tripole pattern relates to the strength of the oceanic gyres in the north Atlantic, which are partly driven by wind-stress on the ocean surface (Häkkinen et al., 2011). In the configuration of Fig. 7A, cyclonic circulation and cold SSTs prevail south of Greenland, while heat is transferred from ocean to atmosphere (Häkkinen et al., 2011). The tripole pattern can occur already in late winter and early spring and is known to precede the summertime SEA pattern (Fig. 5I) (Gastineau and Frankignoul, 2015; Ossó et al., 2020; Wolf et al., 2020; Beobide-Arsuaga et al., 2023). Spring SST anomalies are particularly strengthened by a two-way coupling between ocean and jet stream. This happens as soon as the north Atlantic jet migrates northward with the change of seasons (Wolf et al., 2020; Ossó et al., 2020). Indeed we see that sharp meridional SST gradients are co-located with jet stream position over the Atlantic (Fig. 7A,D). Strong u300 anomalies are present in week -2 to 0, and show a stronger and narrower Atlantic jet as compared to the broader climatological mean jet (green contours, Fig. 7D). In the case without SST tripole, and without a t2m response

https://doi.org/10.5194/wcd-2023-6
Preprint. Discussion started: 21 February 2023

in week 3-6, the jet is less strong (Fig. 7F). Strong and narrow jets form better waveguides (Manola et al., 2013; White et al., 2022), and in this case precede the QSRW and the t2m response. We therefore deduce that the interplay of SST tripole and Atlantic jet modulates the teleconnection by longitudinally guiding QSRWs from the west Pacific towards Europe.

7 Discussion and conclusion

In this study we have defined a west Pacific Dipole (WPD) index that captures the strength of a dipole SST pattern in the western Pacific. These contrasts in SST occur in both the equatorial and meridional direction, and were shown to relate to changing patterns of deep convection and large-scale SST changes across the Pacific. Specifically, the WPD targets those heating patterns that excite Quasi-Stationary Rossby Waves (QSRW) that potentially affect west and central Europe more than two weeks later. Such teleconnections are known mechanisms for sub-seasonal predictability. Cross-correlations make clear that the emphasis of the WPD is different than, but still relates to, well-known Pacific modes like ENSO and PDO (Fig. 3B,C). Particularly, the positive and negative WPD phases in summer coincide with the strengthening of ENSO (Fig. 6). Also, the index is not overly sensitive to the exact placement of its boxes on the correlation map (Fig. 2). An index based on three components, with one northward box inside the PDO region, led to similar results.

A prominent result of this study is that negative WPD phases have become more frequent over recent decades. In this phase, convection over the Maritime Continent and western north Pacific is enhanced, and that over the central Equatorial Pacific suppressed. Its increased occurrence reflects a long-term shift towards 'La Niña-like' states with stronger equatorial SST gradients, as a consequence of the west Pacific warming relative to the central tropical Pacific. This west Pacific warming mode is thought to be a response to anthropogenic forcing, and to strengthen the Walker circulation (Funk and Hoell, 2015).

Coinciding with the long term SST changes we find that the WPD phase during weeks -2 to 0 becomes an important predictor for the European t2m response in week 3 to 6 (Fig. 4B) (also van Straaten et al., 2023). We diagnose that this summertime Pacific to Euro-Atlantic teleconnection emerged after 1980, which agrees with other studies (O'Reilly et al., 2019; Sun et al., 2022). We should however be cautious about concluding that the teleconnection has been absent before 1980, as it can also relate to data quality, which improved with the advent of satellite observations (Hersbach et al., 2020). Nonetheless, we show that for the period of 1980 till 2021 connectivity is significant, and that the teleconnection pathway can be well understood. Following the heating anomalies, a QSRW develops in week 1 to 2 and consists of known centers of action. These centers span the north American continent (known from Vijverberg and Coumou (2022)), and then extend eastward to encompass a large center south of Greenland, and one over west and central Europe (resembling the known Summer East Alantic (SEA) pattern (Wulff et al., 2017)). An additional center of action is located over eastern Europe and Russia, and has a sign that opposes the sign over west and central Europe (known from Behera et al., 2013; Lee et al., 2017).

Given this significant emergence in recent decades, the teleconnection explains some recent changes in the summer circulation over Europe. The increased frequency of the negative WPD phase, would according to its corresponding QSRW, induce a warming in eastern Europe and Russia. Indeed, high pressure has become more prevalent there (Lee et al., 2017; Kim and Lee, 2022), and the region has seen a very strong increase in heatwaves (Rousi et al., 2022).

https://doi.org/10.5194/wcd-2023-6
Preprint. Discussion started: 21 February 2023

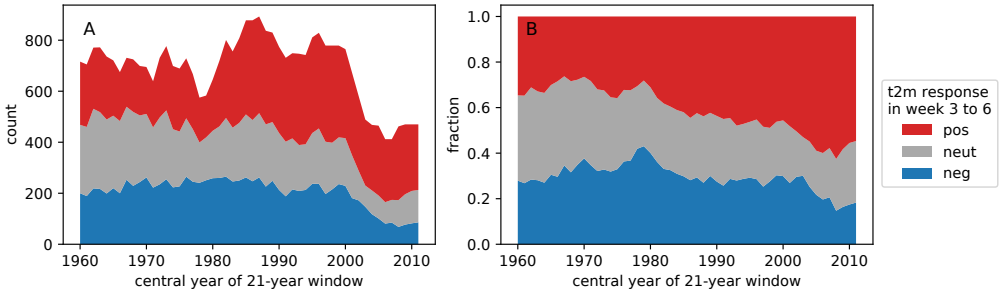

Figure 8. A) Count of positive WPD phases and its resulting t2m responses in a moving window of 21 summer seasons. Positive WPD phases are recorded when the west Pacific Dipole index in week -2 to 0 is in its upper tercile class (thresholds are determined over entire dataset, from 1950-2021). The total count is subdivided into positive WPD phases resulting in negative, neutral or positive t2m anomalies in week 3 to 6 (respectively: blue, grey and red). Tercile thresholds for t2m are re-computed in each window (as in Fig. 4). B) As panel A, but presented as a fraction of the total count.

As the eastern European center of action opposes the western one, we would expect that the increased occurrence of negative WPD induces a relative cooling over western Europe, particularly because after 2000 the increase of negative WPD also happens at the expense of positive WPD (Fig. 4A). This is however not observed, as also in west and central Europe temperatures and surface pressure are increasing (Boe et al., 2020; van Oldenborgh et al., 2022). Still our findings shed some light on these seemingly contradictory results. The QSRW with high pressure over western Europe (following positive WPD phases) is namely found to be modulated by the situation in the Atlantic. A combination of SST tripole and a strong and narrow jet in the north Atlantic allow the QSRW to reach western Europe. Prominent in this modulation are the relatively cold SSTs south of Greenland (agreeing with Fuentes-Franco et al., 2022). Such relatively cold SSTs have become prevalent since the 1980's (Chemke et al., 2020). This could imply that although the total count of positive WPD phases decreases (Fig. 4A and Fig. 8A), those that do occur are more likely to generate a QSRW that reaches western Europe. This seems to be confirmed by the increased fraction of positive WPD phases resulting in positive t2m anomalies (red, Fig. 8B) as compared to those resulting in neutral or negative t2m anomalies (grey and blue, Fig. 8B).

We suggest that the interplay between long-term Pacific changes and long-term north Atlantic changes be researched further. Relevant in this interplay, are the cold north Atlantic SSTs, which can become more prevalent if Atlantic meridional overturning circulation slows down. Climate model experiments suggest that such slowdown might follow from further anthropogenic forcing and can generate a summertime high pressure response not far from the UK (Haarsma et al., 2015; Rousi et al., 2021). Relevant for the interplay are also long term changes that potentially affect jet stream strength, like Arctic amplification and aerosols (Coumou et al., 2018; Dong et al., 2022).

Such research should probably not be conducted with numerical climate models only. Our analysis namely emphasized features that climate models have difficulty capturing. One is the strengthening of equatorial gradients in Pacific SST, which we detected as the increase of negative WPD phases. We know that climate models are unable to reproduce the observed strengthening, and simulate a weakening instead (Funk and Hoell, 2015; Wills et al., 2022; Seager et al., 2022; Lee et al.,

https://doi.org/10.5194/wcd-2023-6
Preprint. Discussion started: 21 February 2023

2022). Worrying is that even with prescribed SSTs, climate models fail to reproduce the associated dynamical response: an increased prevalence of high pressure over western and eastern Europe (Boe et al., 2020). It thus appears that climate models do not represent the detected QSRWs well. A similar failure to represent the teleconnection pathway happens in the ECMWF model, despite being initialized with observed SSTs (van Straaten et al., 2023).

Resolving these issues is challenging because the shortcomings of climate models force us to use observations or reanalysis products. These are of limited length, with few independent samples as a result. It is also challenging because a full theoretical understanding of QSRWs on different space and time scales does not exist (White et al., 2022). We hope that the targeted WPD index provides future diagnostic studies with a starting point. An improved representation of the Pacific-to-Europe connection in weather and climate models has a lot to offer. One is a better projection of European summer extremes (van Oldenborgh et al., 2022). The other is a conditional opportunity to forecast European summer circulation more than two weeks in advance (Mariotti et al., 2020; van Straaten et al., 2023).

Code and data availability. The ERA5 reanalysis can be obtained from the Copernicus Climate Data Store https://cds.climate.copernicus.eu. The PDO index can be accessed at https://oceanview.pfeg.noaa.gov/erddap/tabledap/cciea_OC_PDO.html. The relative ENSO indices can be accessed at the KNMI Climate Explorer https://climexp.knmi.nl/selectindex.cgi. Python code used to conduct this study can be accessed at https://github.com/chiemvs/telegates

Author contributions. All authors conceptualized the research and designed the experiments. CvS conducted the analysis, created visualizations and wrote the initial draft. All authors contributed through reviewing and editing.

Competing interests. The authors declare that they have no conflict of interest.

Acknowledgements. This study is part of the open research programme Aard- en Levenswetenschappen, project number ALWOP.395, which is financed by the Dutch Research Council (NWO). We thank maintainers and funders of the BAZIS cluster at VU Amsterdam for computational resources. D.C. acknowledges support from a NWO Vidi grant (Persistent Summer Extremes "PERSIST"). This research was partly funded from the European Union's Horizon 2020 research and innovation program under grant agreements 101003469 and 820970.

https://doi.org/10.5194/wcd-2023-6
Preprint. Discussion started: 21 February 2023

References

Behera, S., Ratnam, J. V., Masumoto, Y., and Yamagata, T.: Origin of extreme summers in Europe: the Indo-Pacific connection, Climate dynamics, 41, 663–676, https://doi.org/10.1007/s00382-012-1524-8, 2013.

Benjamini, Y. and Hochberg, Y.: Controlling the false discovery rate: a practical and powerful approach to multiple testing, Journal of the Royal statistical society: series B (Methodological), 57, 289–300, https://doi.org/https://doi.org/10.1175/BAMS-D-15-00267.1, 1995.

Beobide-Arsuaga, G., Düsterhus, A., Müller, W. A., Barnes, E. A., and Baehr, J.: Spring Regional Sea Surface Temperatures as a Precursor of European Summer Heatwaves, Geophysical Research Letters, 50, e2022GL100 727, https://doi.org/https://doi.org/10.1029/2022GL100727, e2022GL100727 2022GL100727, 2023.

Bjerknes, J.: Atmospheric teleconnections from the equatorial Pacific, Monthly weather review, 97, 163–172, https://doi.org/10.1175/1520-0493(1969)097<0163:ATFTEP>2.3.CO;2, 1969.

Boe, J., Terray, L., Moine, M.-P., Valcke, S., Bellucci, A., Drijfhout, S., Haarsma, R., Lohmann, K., Putrasahan, D. A., Roberts, C., et al.: Past long-term summer warming over western Europe in new generation climate models: role of large-scale atmospheric circulation, Environmental Research Letters, 15, 084 038, https://doi.org/10.1088/1748-9326/ab8a89, 2020.

Branstator, G.: Long-lived response of the midlatitude circulation and storm tracks to pulses of tropical heating, Journal of Climate, 27, 8809–8826, https://doi.org/10.1175/JCLI-D-14-00312.1, 2014.

Branstator, G. and Teng, H.: Tropospheric waveguide teleconnections and their seasonality, Journal of the Atmospheric Sciences, 74, 1513–1532, https://doi.org/10.1175/JAS-D-16-0305.1, 2017.

Buizza, R. and Leutbecher, M.: The forecast skill horizon, Quarterly Journal of the Royal Meteorological Society, 141, 3366–3382, https://doi.org/10.1002/qj.2619, 2015.

Cassou, C.: Intraseasonal interaction between the Madden–Julian oscillation and the North Atlantic Oscillation, Nature, 455, 523, https://doi.org/10.1038/nature07286, 2008.

Cassou, C., Terray, L., and Phillips, A. S.: Tropical Atlantic influence on European heat waves, Journal of climate, 18, 2805–2811, https://doi.org/10.1175/JCLI3506.1, 2005.

Chemke, R., Zanna, L., and Polvani, L. M.: Identifying a human signal in the North Atlantic warming hole, Nature communications, 11, 1–7, https://doi.org/10.1038/s41467-020-15285-x, 2020.

Christidis, N., Jones, G. S., and Stott, P. A.: Dramatically increasing chance of extremely hot summers since the 2003 European heatwave, Nature Climate Change, 5, 46–50, https://doi.org/10.1038/nclimate2468, 2015.

Coumou, D., Di Capua, G., Vavrus, S., Wang, L., and Wang, S.: The influence of Arctic amplification on mid-latitude summer circulation, Nature Communications, 9, 1–12, https://doi.org/10.1038/s41467-018-05256-8, 2018.

Di Capua, G., Runge, J., Donner, R. V., van den Hurk, B., Turner, A. G., Vellore, R., Krishnan, R., and Coumou, D.: Dominant patterns of interaction between the tropics and mid-latitudes in boreal summer: causal relationships and the role of timescales, Weather and Climate Dynamics, 1, 519–539, https://doi.org/10.5194/wcd-1-519-2020, 2020.

Ding, Q., Wang, B., Wallace, J. M., and Branstator, G.: Tropical–extratropical teleconnections in boreal summer: Observed interannual variability, Journal of Climate, 24, 1878–1896, https://doi.org/10.1175/2011JCLI3621.1, 2011.

Dong, B., Sutton, R. T., Shaffrey, L., and Harvey, B.: Recent decadal weakening of the summer Eurasian westerly jet attributable to anthropogenic aerosol emissions, Nature Communications, 13, 1148, https://doi.org/10.1038/s41467-022-28816-5, 2022.

https://doi.org/10.5194/wcd-2023-6
Preprint. Discussion started: 21 February 2023

Fuentes-Franco, R. and Koenigk, T.: Identifying remote sources of interannual variability for summer precipitation over Nordic European countries tied to global teleconnection wave patterns, Tellus A: Dynamic Meteorology and Oceanography, 72, 1–15, https://doi.org/10.1080/16000870.2020.1764303, 2020.

Fuentes-Franco, R., Koenigk, T., Docquier, D., Graef, F., and Wyser, K.: Exploring the influence of the North Pacific Rossby wave sources on the variability of summer atmospheric circulation and precipitation over the Northern Hemisphere, Climate Dynamics, pp. 1–15, https://doi.org/10.1007/s00382-022-06194-4, 2022.

Funk, C., Harrison, L., Shukla, S., Pomposi, C., Galu, G., Korecha, D., Husak, G., Magadzire, T., Davenport, F., Hillbruner, C., et al.: Examining the role of unusually warm Indo-Pacific sea-surface temperatures in recent African droughts, Quarterly Journal of the Royal Meteorological Society, 144, 360–383, https://doi.org/10.1002/qj.3266, 2018.

Funk, C. C. and Hoell, A.: The leading mode of observed and CMIP5 ENSO-residual sea surface temperatures and associated changes in Indo-Pacific climate, Journal of Climate, 28, 4309–4329, https://doi.org/10.1175/JCLI-D-14-00334.1, 2015.

Gastineau, G. and Frankignoul, C.: Influence of the North Atlantic SST variability on the atmospheric circulation during the twentieth century, Journal of Climate, 28, 1396–1416, https://doi.org/10.1175/JCLI-D-14-00424.1, 2015.

Haarsma, R. J., Selten, F. M., and Drijfhout, S. S.: Decelerating Atlantic meridional overturning circulation main cause of future west European summer atmospheric circulation changes, Environmental Research Letters, 10, 094 007, https://doi.org/10.1088/1748-9326/10/9/094007, 2015.

Henderson, S. A., Maloney, E. D., and Son, S.-W.: Madden–Julian oscillation Pacific teleconnections: The impact of the basic state and MJO representation in general circulation models, Journal of Climate, 30, 4567–4587, https://doi.org/10.1175/JCLI-D-16-0789.1, 2017.

Hersbach, H., Bell, B., Berrisford, P., Hirahara, S., Horányi, A., Muñoz-Sabater, J., Nicolas, J., Peubey, C., Radu, R., Schepers, D., et al.: The ERA5 global reanalysis, Quarterly Journal of the Royal Meteorological Society, 146, 1999–2049, https://doi.org/10.1002/qj.3803, 2020.

Hoskins, B. J. and Ambrizzi, T.: Rossby wave propagation on a realistic longitudinally varying flow, Journal of Atmospheric Sciences, 50, 1661–1671, https://doi.org/10.1175/1520-0469(1993)050<1661:RWPOAR>2.0.CO;2, 1993.

Hoskins, B. J. and Karoly, D. J.: The steady linear response of a spherical atmosphere to thermal and orographic forcing, Journal of the atmospheric sciences, 38, 1179–1196, https://doi.org/10.1175/1520-0469(1981)038<1179:TSLROA>2.0.CO;2, 1981.

Huang, B., Thorne, P. W., Banzon, V. F., Boyer, T., Chepurin, G., Lawrimore, J. H., Menne, M. J., Smith, T. M., Vose, R. S., and Zhang, H.-M.: Extended reconstructed sea surface temperature, version 5 (ERSSTv5): upgrades, validations, and intercomparisons, Journal of Climate, 30, 8179–8205, https://doi.org/10.1175/JCLI-D-16-0836.1, 2017.

Häkkinen, S., Rhines, P. B., and Worthen, D. L.: Atmospheric Blocking and Atlantic Multidecadal Ocean Variability, Science, 334, 655–659, https://doi.org/10.1126/science.1205683, 2011.

Jong, B.-T., Ting, M., Seager, R., and Anderson, W. B.: ENSO teleconnections and impacts on US summertime temperature during a multiyear La Niña life cycle, Journal of Climate, 33, 6009–6024, https://doi.org/10.1175/JCLI-D-19-0701.1, 2020.

Kim, D. W. and Lee, S.: The Role of Latent Heating Anomalies in Exciting the Summertime Eurasian Circulation Trend Pattern and High Surface Temperature, Journal of Climate, 35, 801–814, https://doi.org/10.1175/JCLI-D-21-0392.1, 2022.

Lee, M.-H., Lee, S., Song, H.-J., and Ho, C.-H.: The recent increase in the occurrence of a boreal summer teleconnection and its relationship with temperature extremes, Journal of Climate, 30, 7493–7504, https://doi.org/10.1175/JCLI-D-16-0094.1, 2017.

Lee, S., L'Heureux, M., Wittenberg, A. T., Seager, R., O'Gorman, P. A., and Johnson, N. C.: On the future zonal contrasts of equatorial Pacific climate: Perspectives from Observations, Simulations, and Theories, npj Climate and Atmospheric Science, 5, 82, https://doi.org/10.1038/s41612-022-00301-2, 2022.

https://doi.org/10.5194/wcd-2023-6
Preprint. Discussion started: 21 February 2023

Lim, Y.-K., Cullather, R. I., Nowicki, S. M., and Kim, K.-M.: Inter-relationship between subtropical Pacific sea surface temperature, Arctic sea ice concentration, and North Atlantic Oscillation in recent summers, Scientific reports, 9, 1–11, https://doi.org/10.1038/s41598-019-39896-7, 2019.

Liu, Z. and Alexander, M.: Atmospheric bridge, oceanic tunnel, and global climatic teleconnections, Reviews of Geophysics, 45, https://doi.org/10.1029/2005RG000172, 2007.

Ma, Q. and Franzke, C. L.: The role of transient eddies and diabatic heating in the maintenance of European heat waves: a nonlinear quasi-stationary wave perspective, Climate Dynamics, 56, 2983–3002, https://doi.org/10.1007/s00382-021-05628-9, 2021.

Manola, I., Selten, F., de Vries, H., and Hazeleger, W.: "Waveguidability" of idealized jets, Journal of Geophysical Research: Atmospheres, 118, 10–432, https://doi.org/10.1002/jgrd.50758, 2013.

Mantua, N. J., Hare, S. R., Zhang, Y., Wallace, J. M., and Francis, R. C.: A Pacific interdecadal climate oscillation with impacts on salmon production, Bulletin of the american Meteorological Society, 78, 1069–1080, https://doi.org/10.1175/1520-0477(1997)078<1069:APICOW>2.0.CO;2, 1997.

Mariotti, A., Baggett, C., Barnes, E. A., Becker, E., Butler, A., Collins, D. C., Dirmeyer, P. A., Ferranti, L., Johnson, N. C., Jones, J., et al.: Windows of Opportunity for Skillful Forecasts Subseasonal to Seasonal and Beyond, Bulletin of the American Meteorological Society, 101, E608–E625, https://doi.org/10.1175/BAMS-D-18-0326.1, 2020.

Mayer, K. and Barnes, E. A.: Subseasonal Forecasts of Opportunity Identified by an Explainable Neural Network, Geophysical Research Letters, 48, e2020GL092 092, https://doi.org/10.1029/2020GL092092, 2021.

Mayer, K. J. and Barnes, E. A.: Quantifying the Effect of Climate Change on Midlatitude Subseasonal Prediction Skill Provided by the Tropics, Geophysical Research Letters, 49, e2022GL098 663, https://doi.org/10.1029/2022GL098663, 2022.

Newman, M., Alexander, M. A., Ault, T. R., Cobb, K. M., Deser, C., Di Lorenzo, E., Mantua, N. J., Miller, A. J., Minobe, S., Nakamura, H., et al.: The Pacific decadal oscillation, revisited, Journal of Climate, 29, 4399–4427, https://doi.org/10.1175/JCLI-D-15-0508.1, 2016.

O'Reilly, C. H., Woollings, T., Zanna, L., and Weisheimer, A.: An interdecadal shift of the extratropical teleconnection from the tropical Pacific during boreal summer, Geophysical Research Letters, 46, 13 379–13 388, https://doi.org/10.1029/2019GL084079, 2019.

Ossó, A., Sutton, R., Shaffrey, L., and Dong, B.: Development, amplification and decay of Atlantic/European summer weather patterns linked to spring North Atlantic sea surface temperatures, Journal of Climate, 33, 5939–5951, https://doi.org/10.1175/JCLI-D-19-0613.1, 2020.

O'Reilly, C. H., Woollings, T., Zanna, L., and Weisheimer, A.: The Impact of Tropical Precipitation on Summertime Euro-Atlantic Circulation via a Circumglobal Wave Train, Journal of Climate, 31, 6481–6504, https://doi.org/10.1175/JCLI-D-17-0451.1, 2018.

Quinting, J. and Vitart, F.: Representation of Synoptic-Scale Rossby Wave Packets and Blocking in the S2S Prediction Project Database, Geophysical Research Letters, 46, 1070–1078, https://doi.org/10.1029/2018GL081381, 2019.

Röthlisberger, M., Frossard, L., Bosart, L. F., Keyser, D., and Martius, O.: Recurrent synoptic-scale Rossby wave patterns and their effect on the persistence of cold and hot spells, Journal of Climate, 32, 3207–3226, https://doi.org/10.1175/JCLI-D-18-0664.1, 2019.

Rousi, E., Selten, F., Rahmstorf, S., and Coumou, D.: Changes in North Atlantic atmospheric circulation in a warmer climate favor winter flooding and summer drought over Europe, Journal of Climate, 34, 2277–2295, https://doi.org/10.1175/JCLI-D-20-0311.1, 2021.

Rousi, E., Kornhuber, K., Beobide-Arsuaga, G., Luo, F., and Coumou, D.: Accelerated western European heatwave trends linked to more-persistent double jets over Eurasia, Nature communications, 13, 1–11, https://doi.org/10.1038/s41467-022-31432-y, 2022.

Sardeshmukh, P. D. and Hoskins, B. J.: The generation of global rotational flow by steady idealized tropical divergence, Journal of the Atmospheric Sciences, 45, 1228–1251, https://doi.org/10.1175/1520-0469(1988)045<1228:TGOGRF>2.0.CO;2, 1988.

https://doi.org/10.5194/wcd-2023-6
Preprint. Discussion started: 21 February 2023

Schneidereit, A., Schubert, S., Vargin, P., Lunkeit, F., Zhu, X., Peters, D. H., and Fraedrich, K.: Large-scale flow and the long-lasting blocking high over Russia: Summer 2010, Monthly Weather Review, 140, 2967–2981, https://doi.org/10.1175/MWR-D-11-00249.1, 2012.

Schubert, S., Wang, H., and Suarez, M.: Warm season subseasonal variability and climate extremes in the Northern Hemisphere: The role of stationary Rossby waves, Journal of Climate, 24, 4773–4792, https://doi.org/10.1175/JCLI-D-10-05035.1, 2011.

Schubert, S. D., Wang, H., Koster, R. D., Suarez, M. J., and Groisman, P. Y.: Northern Eurasian heat waves and droughts, Journal of Climate, 27, 3169–3207, https://doi.org/10.1175/JCLI-D-13-00360.1, 2014.

Seager, R., Henderson, N., and Cane, M.: Persistent Discrepancies between Observed and Modeled Trends in the Tropical Pacific Ocean, Journal of Climate, 35, 4571 – 4584, https://doi.org/10.1175/JCLI-D-21-0648.1, 2022.

Stan, C., Straus, D. M., Frederiksen, J. S., Lin, H., Maloney, E. D., and Schumacher, C.: Review of tropical-extratropical teleconnections on intraseasonal time scales, Reviews of Geophysics, 55, 902–937, https://doi.org/10.1002/2016RG000538, 2017.

Sun, X., Ding, Q., Wang, S.-Y. S., Topál, D., Li, Q., Castro, C., Teng, H., Luo, R., and Ding, Y.: Enhanced jet stream waviness induced by suppressed tropical Pacific convection during boreal summer, Nature Communications, 13, 1–10, https://doi.org/10.1038/s41467-022-28911-7, 2022.

Teng, H. and Branstator, G.: Amplification of waveguide teleconnections in the boreal summer, Current Climate Change Reports, 5, 421–432, https://doi.org/10.1007/s40641-019-00150-x, 2019.

Ting, M.: Maintenance of northern summer stationary waves in a GCM, Journal of the atmospheric sciences, 51, 3286–3308, https://doi.org/10.1175/1520-0469(1994)051<3286:MONSSW>2.0.CO;2, 1994.

Trenberth, K. E. and Stepaniak, D. P.: Indices of el Niño evolution, Journal of climate, 14, 1697–1701, https://doi.org/10.1175/1520-0442(2001)014<1697:LIOENO>2.0.CO;2, 2001.

Trenberth, K. E., Branstator, G. W., Karoly, D., Kumar, A., Lau, N.-C., and Ropelewski, C.: Progress during TOGA in understanding and modeling global teleconnections associated with tropical sea surface temperatures, Journal of Geophysical Research: Oceans, 103, 14 291–14 324, https://doi.org/10.1029/97JC01444, 1998.

van Oldenborgh, G. J., Hendon, H., Stockdale, T., L'Heureux, M., De Perez, E. C., Singh, R., and Van Aalst, M.: Defining El Niño indices in a warming climate, Environmental research letters, 16, 044 003, https://doi.org/10.1088/1748-9326/abe9ed, 2021.

van Oldenborgh, G. J., Wehner, M. F., Vautard, R., Otto, F. E. L., Seneviratne, S. I., Stott, P. A., Hegerl, G. C., Philip, S. Y., and Kew, S. F.: Attributing and projecting heatwaves is hard: We can do better, Earth's Future, 10, e2021EF002 271, https://doi.org/10.1029/2021EF002271, e2021EF002271 2021EF002271, 2022.

van Straaten, C., Whan, K., Coumou, D., van den Hurk, B., and Schmeits, M.: The influence of aggregation and statistical post-processing on the subseasonal predictability of European temperatures, Quarterly Journal of the Royal Meteorological Society, 146, 2654–2670, https://doi.org/10.1002/qj.3810, 2020.

van Straaten, C., Whan, K., Coumou, D., van den Hurk, B., and Schmeits, M.: Using explainable machine learning forecasts to discover sub-seasonal drivers of high summer temperatures in western and central Europe, Monthly Weather Review, 150, 1115–1134, https://doi.org/10.1175/MWR-D-21-0201.1, 2022.

van Straaten, C., Whan, K., Coumou, D., van den Hurk, B., and Schmeits, M.: Correcting sub-seasonal forecast errors with an explainable ANN to understand misrepresented sources of predictability of European summer temperatures, Artificial Intelligence for the Earth Systems, in revision, 2023.

Vijverberg, S. and Coumou, D.: The role of the Pacific Decadal Oscillation and ocean-atmosphere interactions in driving US temperature predictability, npj Climate and Atmospheric Science, 5, 1–11, https://doi.org/10.1038/s41612-022-00237-7, 2022.

https://doi.org/10.5194/wcd-2023-6
Preprint. Discussion started: 21 February 2023

Vitart, F.: Madden—Julian oscillation prediction and teleconnections in the S2S database, Quarterly Journal of the Royal Meteorological Society, 143, 2210–2220, https://doi.org/10.1002/qj.3079, 2017.

Vitart, F. and Robertson, A. W.: The sub-seasonal to seasonal prediction project (S2S) and the prediction of extreme events, npj Climate and Atmospheric Science, 1, 3, https://doi.org/10.1038/s41612-018-0013-0, 2018.

Wheeler, M. C., Zhu, H., Sobel, A. H., Hudson, D., and Vitart, F.: Seamless precipitation prediction skill comparison between two global models, Quarterly Journal of the Royal Meteorological Society, 143, 374–383, https://doi.org/10.1002/qj.2928, 2017.

White, R. H., Kornhuber, K., Martius, O., and Wirth, V.: From Atmospheric Waves to Heatwaves: A Waveguide Perspective for Understanding and Predicting Concurrent, Persistent, and Extreme Extratropical Weather, Bulletin of the American Meteorological Society, 103, E923–E935, https://doi.org/10.1175/BAMS-D-21-0170.1, 2022.

Wills, R. C., Dong, Y., Proistosecu, C., Armour, K. C., and Battisti, D. S.: Systematic climate model biases in the large-scale patterns of recent sea-surface temperature and sea-level pressure change, Geophysical Research Letters, p. e2022GL100011, https://doi.org/10.1029/2022GL100011, 2022.

Wirth, V., Riemer, M., Chang, E. K., and Martius, O.: Rossby Wave Packets on the Midlatitude Waveguide—A Review, Monthly Weather Review, 146, 1965–2001, https://doi.org/10.1175/MWR-D-16-0483.1, 2018.

Wolf, G., Brayshaw, D. J., Klingaman, N. P., and Czaja, A.: Quasi-stationary waves and their impact on European weather and extreme events, Quarterly Journal of the Royal Meteorological Society, 144, 2431–2448, https://doi.org/10.1002/qj.3310, 2018.

Wolf, G., Czaja, A., Brayshaw, D., and Klingaman, N.: Connection between sea surface anomalies and atmospheric quasi-stationary waves, Journal of Climate, 33, 201–212, https://doi.org/10.1175/JCLI-D-18-0751.1, 2020.

Wu, Z. and Lin, H.: Interdecadal variability of the ENSO–North Atlantic Oscillation connection in boreal summer, Quarterly Journal of the Royal Meteorological Society, 138, 1668–1675, https://doi.org/10.1002/qj.1889, 2012.

Wulff, C. O., Greatbatch, R. J., Domeisen, D. I., Gollan, G., and Hansen, F.: Tropical forcing of the Summer East Atlantic pattern, Geophysical Research Letters, 44, 11–166, https://doi.org/10.1002/2017GL075493, 2017.